Letter

Reconciling Kubo and Keldysh approaches to Fermi-sea-dependent nonequilibrium observables: Application to spin Hall current and spin-orbit torque in spintronics

Simão M. João,[1] Marko D. Petrović,[2] J. M. Viana Parente Lopes,[3] Aires Ferreira,[4,*] and Branislav K. Nikolić[2,†]

[1]*Department of Materials, Imperial College London, London SW7 2AZ, United Kingdom*

[2]*Department of Physics and Astronomy, University of Delaware, Newark, Delaware 19716, USA*

[3]*Centro de Física das Universidades do Minho e Porto and Departamento de Física e Astronomia, Faculdade de Ciências, Universidade do Porto, 4169-007 Porto, Portugal*

[4]*Department of Physics, University of York, York YO10 5DD, United Kingdom*

(Received 5 November 2024; revised 24 November 2025; accepted 26 November 2025; published 24 December 2025)

Quantum transport studies of spin-dependent phenomena in solids commonly employ the Kubo or Keldysh formulas for the nonequilibrium density operator in the steady-state linear-response regime. Its trace with operators of interest, such as the spin density, spin current density, and so on, gives expectation values of experimentally accessible observables. As is well known, for *local* observables, these formulas require summing over the manifolds of *both* Fermi-surface and Fermi-sea states. However, the significantly different results yielded by the two formulations when applied to the same system have ignited vigorous debates. Here, we revisit this problem using an infinite-size graphene system with proximity-induced spin-orbit and magnetic exchange effects as a test bed. By considering such system as being composed of central active region in between two semi-infinite leads, in the spirit of the Landauer setup for quantum transport, we prove the *numerically exact equivalence* of the Kubo and Keldysh approaches via the computation of spin Hall current density and spin-orbit torque in both clean and disordered limits. The key to reconciling the two approaches is the numerical frameworks we put forward for (i) evaluation of the Kubo(-Bastin) formula for a system attached to semi-infinite leads, which ensures a *continuous energy spectrum* and evades the need for commonly used phenomenological broadening otherwise responsible for ambiguities, and (ii) proper evaluation of the Fermi-sea term in the Keldysh approach, which *must* include the voltage drop across the central active region even if it is disorder free.

DOI: 10.1103/zwqs-gpr4

The density (or state or statistical) operator [1] is the central concept of quantum statistical mechanics. The operator and its representation—the density matrix—in some basis of the Hilbert space are essential conditions to describe equilibrium quantum systems at finite temperature [2], as well as out-of-equilibrium systems driven by steady or time-dependent external fields. The density operator also plays a crucial role in describing the transition between nonequilibrium and equilibrium states [3], as well as in zero-temperature quantum mechanics [4] and quantum information science, where it describes decoherence (i.e., the decay of the off-diagonal elements of the density matrix in some preferred basis [5]), and eventually quantum-to-classical transitions [5,6]. From the knowledge of the density matrix $\hat{\rho}$, the expectation value of a physical observable represented by a Hermitian operator $\hat{O}$ is obtained from $O = \mathrm{Tr}[\hat{\rho}\,\hat{O}]$. The density matrix in equilibrium is unambiguously specified by the Boltzmann and Gibbs prescription. A textbook example [2] is the grand canonical ensemble $\hat{\rho}_{\mathrm{eq}} = \sum_n f(E_n)|E_n\rangle\langle E_n|$ for noninteracting fermions with single-particle energy levels E_n, occupied according to the Fermi-Dirac distribution function $f(E)$, and with the corresponding eigenstates $|E_n\rangle$ of a fermionic Hamiltonian. By contrast, there is no unique procedure to obtain the density matrix of steady-state [7,8] or time-dependent [9–12] nonequilibrium systems and for arbitrary strength of the driving field [7], while including their many-body interactions [12].

Nonetheless, in problems of noninteracting electrons driven by weak external fields, linear-response theory of Kubo [13] or Keldysh Green's functions (GFs) [14,15] makes it possible to construct a *universal* expression for $\hat{\rho}^{\mathrm{neq}}$ that is expressed in terms of the retarded GF involving the Hamiltonian of the system in *equilibrium*, $\hat{H}$. For example, in the case of the Kubo formula [13], and using Bastin *et al.* [16] formulation in terms of GFs, the steady-state $\hat{\rho}^{\mathrm{neq}}$ (at zero temperature for simplicity) is given by

$$\hat{\rho}^{\mathrm{neq}}_{\mathrm{Kubo}} = \hat{\rho}^{\mathrm{surf}}_{\mathrm{Kubo}} + \hat{\rho}^{\mathrm{sea}}_{\mathrm{Kubo}}, \tag{1a}$$

$$\hat{\rho}^{\mathrm{surf}}_{\mathrm{Kubo}} = \frac{4eE_x}{h}\mathrm{Re}[\mathrm{Im}\,\hat{G}\,\hat{v}_{\mathrm{x}}\,\mathrm{Im}\,\hat{G}], \tag{1b}$$

$$\hat{\rho}^{\mathrm{sea}}_{\mathrm{Kubo}} = \frac{2eE_x}{h}\int dE\, f(E)\mathrm{Re}[(\hat{G}^r - \hat{G}^a)\hat{v}_{\mathrm{x}}\,\partial_E\,\mathrm{Re}\,\hat{G}], \tag{1c}$$

where $\partial_E \equiv \partial/\partial E$ and E_x is the electric field strength (assumed to point along the $\hat{x}$ axis). Note that several decompositions [17] into $\hat{\rho}^{\mathrm{sea}}_{\mathrm{Kubo}}$ and $\hat{\rho}^{\mathrm{surf}}_{\mathrm{Kubo}}$, governed by the Fermi-sea and Fermi-surface states, respectively, have been used

*Contact author: aires.ferreira@york.ac.uk

†Contact author: bnikolic@udel.edu

historically [18–22]. Here, we employ the specific "symmetrized decomposition" of Ref. [21] ensuring no overlap between the two terms, while also using $\hat{\rho}^{\text{surf}}_{\text{Kubo}}$ as the Kubo-Greenwood form [23,24] which is advantageous for comparison with Keldysh Eq. (4b). The retarded (r) GF standardly used in Eq. (1) is given by

$$\hat{G}^r = [E - \hat{H} + i\eta]^{-1}, \tag{2}$$

where $\hat{G}^a = (\hat{G}^r)^\dagger$ is the advanced GF, $\text{Im}\,\hat{G} = (\hat{G}^r - \hat{G}^a)/2i$, $\text{Re}\,\hat{G} = (\hat{G}^r + \hat{G}^a)/2$, $\hat{\mathbf{v}} = [\hat{\mathbf{r}}, \hat{H}]/i\hbar$ is the velocity operator, and $\hat{\mathbf{r}}$ is the position operator. In most practical applications employing atomistic models [25,26], $\hat{H}$ is either a generic symmetry-allowed [27–30] or first-principles-derived [31–34] tight-binding Hamiltonian on a *finite* lattice with *periodic* boundary conditions. The parameter η (formally an infinitesimal) is required to define $\hat{G}^{r,a}$ by avoiding poles on the real axis [35], with the limit $\eta \to 0$ taken explicitly in analytical approaches [36–40]. However, in numerics, η must remain nonzero due to the discreteness of energy levels [30,41,42], and it can be reduced only at the computational expense of handling larger systems or averaging over random twisted boundary conditions [43]. Physically, a finite η was initially interpreted as mimicking the effect of uncorrelated inelastic scattering processes, thereby defining a phenomenological dephasing timescale $\tau_\phi = \hbar/\eta$ [44]. Later on, η has often been interpreted [21,31] as a homogeneous broadening due to scattering from short-range impurities, but disorder should be explicitly introduced as a term in $\hat{H}$ [such as through ε_i in Eq. (5)] to capture the crucial vertex corrections in $\hat{\rho}^{\text{neq}}_{\text{Kubo}}$ as is well known from diagrammatic theory [36–40,45]. Recently, inspired by the success of approximation theory [46,47], a more practical and accurate interpretation has arisen, where η is seen as an energy resolution that determines how close finite-size spectral simulations are to describing genuine thermodynamic behavior [25,48–50].

The Keldysh formalism [14,15] is applicable beyond the linear-response regime by employing additional GFs. Its fundamental quantities are the retarded $\hat{G}^r(t,t')$ and the lesser $\hat{G}^<(t,t')$ GFs describing the density of available quantum states and how electrons occupy those states, respectively. The diagonal-in-time component of the latter yields the time-dependent nonequilibrium density matrix according to $\hat{\rho}^{\text{neq}}_{\text{Keldysh}}(t) = \frac{\hbar}{i}\hat{G}^<(t,t)$ [9]. In steady-state out-of-equilibrium scenarios, all quantities depend only on the difference $t - t'$, so that after a Fourier transformation in the energy domain E, $\hat{G}^<(E)$ yields the Keldysh formula for the nonequilibrium density matrix, $\hat{\rho}^{\text{neq}}_{\text{Keldysh}} = \frac{1}{2\pi i}\int dE\,\hat{G}^<(E)$. This formula is widely used in computational quantum transport [51] studies of two- [52–56] or multiterminal [57,58] Landauer setups [23,41,51,59–63], where a finite-length central active (CA) region, as in Fig. 1, is coupled to macroscopic Fermi-liquid reservoirs via ideal semi-infinite leads. For instance, in the two-terminal geometry in which the left (L) and right (R) leads terminate into the corresponding reservoirs characterized by the Fermi-Dirac functions, $f_{L,R} = f(E - \mu_{L,R})$, and in the presence of a bias voltage $eV_b = \mu_L - \mu_R$ [here, $\mu_{L,R}$ denotes the electrochemical potential [64] of L or R lead], the lesser GF of the CA region was expressed by Caroli *et al.*

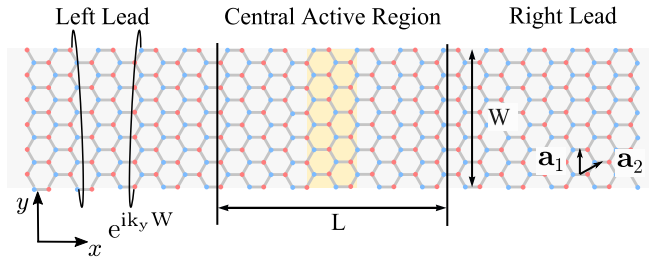

FIG. 1. Doubly proximitized [71] infinite graphene sheet viewed as a two-terminal Landauer setup [23,59–63] for computational quantum transport [51] with its CA region being an armchair nanoribbon (of finite length $L = 40$ Å and width $W = 15$ Å) attached to semi-infinite nanoribbons of the same kind. The nanoribbon is periodically repeated along the y axis to reproduce bulk behavior of an infinite sheet [72]. We employ this setup in the calculation of SH current density (Fig. 2) and SO torque (Fig. 3), within the shaded-in-yellow middle strip, via both Kubo Eq. (1) and Keldysh Eq. (4).

[61] as $\hat{G}^<(E) = i\hat{G}^r(E)[f_L(E)\hat{\Gamma}_L(E) + f_R(E)\hat{\Gamma}_R(E)]\hat{G}^a(E)$. The simplicity of this expression stems from the assumption that many-body interactions are absent in both the CA region [65–67] and the leads [68]. Here, the retarded GF,

$$\hat{G}^r(E) = \left[E - \hat{H} - \hat{\Sigma}^r_L(E) - \hat{\Sigma}^r_R(E)\right]^{-1}, \tag{3}$$

differs from Eq. (2) used in numerical Kubo calculations on systems with periodic boundary conditions [26,27,30–33,58] as it incorporates the leads through their self-energies [51,69,70] $\hat{\Sigma}^r_{L,R}(E)$. They define the level broadening operators, $\hat{\Gamma}_{L,R}(E) = i[\hat{\Sigma}^r_{L,R}(E) - \hat{\Sigma}^a_{L,R}(E)]$, quantifying the electron escape rate into the leads.

The Keldysh formula is valid in the nonlinear regime (i.e., for large V_b) [52,56,73]. Thus, to compare it with the Kubo Eq. (1), we assume small $eV_b \ll E_F$, where E_F is the Fermi energy, leading to $f_L - f_R \approx eV_b\,\delta(E - E_F)$ at zero temperature. In such a linear-response limit, $\hat{\rho}^{\text{neq}}_{\text{Keldysh}}$ can be decomposed [52,74] as (many other decompositions [17] are possible [75,76])

$$\hat{\rho}^{\text{neq}}_{\text{Keldysh}} = \hat{\rho}^{\text{surf}}_{\text{Keldysh}} + \hat{\rho}^{\text{sea}}_{\text{Keldysh}}, \tag{4a}$$

$$\hat{\rho}^{\text{surf}}_{\text{Keldysh}} = \frac{eV_b}{2\pi}\hat{G}^r\hat{\Gamma}_L\hat{G}^a, \tag{4b}$$

$$\hat{\rho}^{\text{sea}}_{\text{Keldysh}} = -\frac{1}{\pi}\int_{-\infty}^{+\infty} dE\, f_R(E)\,\text{Im}\,\hat{G}_{V_b}(E) + \frac{1}{\pi}\int_{-\infty}^{\infty} dE\, f(E)\,\text{Im}\,\hat{G}(E). \tag{4c}$$

In Eq. (4c) we explicitly subtract the grand canonical density matrix in equilibrium (which is built into Kubo's derivation [13]), $\hat{\rho}_{\text{eq}} = -\frac{1}{\pi}\int_{-\infty}^{\infty} dE\, f(E)\,\text{Im}\,\hat{G}(E)$ expressed in terms of GFs, as commonly done [57,73,77] to remove expectation values that can be nonzero in equilibrium but are experimentally not observed, such as a fieldlike [78,79] component of spin torque [73,77], persistent spin currents [57,80], and persistent charge currents [23] (in the presence of an external magnetic field).

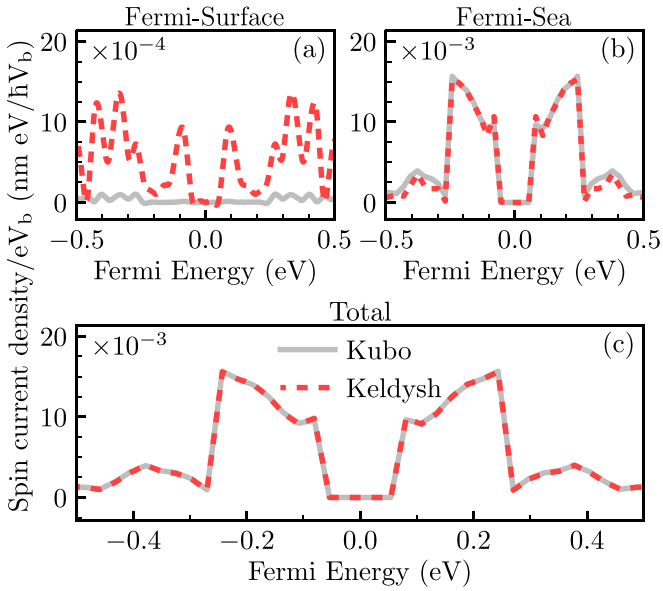

FIG. 2. Spin Hall current density as a function of the Fermi energy. This quantity is obtained by tracing the conventional spin current operator [92] with (a) Fermi-surface, (b) Fermi-sea, and (c) total density matrices in Kubo [Eq. (1)] vs Keldysh [Eq. (4)] approaches employing the same retarded GF [Eq. (3)] of doubly proximitized graphene. The parameters in Eq. (5) are set as $\lambda_{\rm RSO} = J_{\rm sd} = 0.1$ eV and the disorder strength is $D = 0.3$ eV. The spin current density is averaged over 200 disorder configurations. Convergence with respect to k_y-point sampling was also established.

It may seem at first that, because the Kubo Eq. (1) and Keldysh Eq. (4) have quite different functional forms, they describe different scenarios, that is, bulk transport in the former and two-terminal setups in the latter. Nonetheless, the two formulations are general and should lead to the same physical conclusions. Indeed, their equivalence [17] is well established [23,62,63] for longitudinal charge transport observables requiring only $\hat{\rho}^{\rm surf}_{\rm Kubo}$ or $\hat{\rho}^{\rm surf}_{\rm Keldysh}$. However, notably in the context of spin transport, the use of the two formulations has generated widespread confusion and even *divergent conclusions* about the same phenomenon. For example, Ref. [58] compared the spin Hall (SH) current obtained from Keldysh calculations in four-terminal geometry [57] to that of Kubo calculations on periodic lattices, concluding that the Kubo formula is insufficient. Conversely, in spin-orbit (SO) torque calculations, the Keldysh approach apparently predicts [71,81] only the fieldlike (i.e., odd in magnetization [79,82]) component of SO torque $\mathbf{T}_{\rm Keldysh} \equiv \mathbf{T}^o$ in the clean limit, while the Kubo formula yields [83–87] a nonzero value of both $\mathbf{T}^o$ and dampinglike (i.e., even in magnetization [79,82]) SO torque $\mathbf{T}^e$. The even SO torque from the Kubo formula has a well-studied "intrinsic" contribution that is governed [31,83–85] by the Berry curvature of occupied Fermi-sea states and is largely insensitive to a phenomenological η or even to real-space disorder [30]. Thus, $\mathbf{T}_{\rm Keldysh} \neq \mathbf{T}_{\rm Kubo}$, even when both calculations are performed on an identical system, such as the paradigmatic Rashba SO- and exchange-coupled two-dimensional (2D) electron gas [81,84,85]. This in turn has led to the opposite perception, that is, that the Keldysh formula is insufficient. However, $\eta \to 0$ entails $\mathbf{T}^o \to \infty$ [Fig. 3(f)] in Kubo calculations of clean systems, which led to concerns [81] about the use of Kubo Eq. (1) in the absence of extrinsic scattering mechanisms. Additionally, calculations via Kubo Eq. (1) with first-principles Hamiltonian $\hat{H}$ of ferromagnet/heavy-metal bilayers, such as Co/Pt, plugged into GF in Eq. (2) *do not* [31,32] find strongly anisotropic angular features of SO torque, thereby contradicting calculations [79] using Keldysh Eq. (4) with GF in Eq. (2) or experiments [88] on the same Co/Pt system.

In this Letter, we demonstrate the *numerically exact equivalence* between the Kubo and Keldysh approaches by focusing on two paradigmatic examples of coupled spin-charge transport phenomena in spintronics, i.e., the SH effect and the SO torque. We provide a constructive proof of their equivalence by developing numerical frameworks which (i) apply the Kubo(-Bastin) density matrix to two-terminal setups (Fig. 1), via Eq. (3) plugged into Eq. (1), which is an unexplored route in previous studies arriving at *divergent conclusions*, and (ii) properly construct [89] $\hat{\rho}^{\rm sea}_{\rm Keldysh}$ contribution to the Keldysh density matrix [Eq. (4c)], which requires using (a rarely computed [74,79]) $\hat{G}^r_{V_b} = [E - \hat{H} - eU_i - \hat{\Sigma}^r_L - \hat{\Sigma}^r_R]^{-1}$ in Eq. (4c) that includes the voltage drop eU_i across the CA region (Fig. 1). Note that $\hat{G}^r_{V_b}$ is markedly different from $\hat{G}^r$ [Eq. (3)] used in all other terms of Kubo Eq. (1) or Keldysh Eq. (4). Since a voltage drop *cannot* [64] be justified for a clean CA region yielding ballistic charge transport, this also suggests that the computation of local transport quantities always requires the introduction of real-space disorder, even though disorder averaging is often avoided due to the high computational cost of repeated integrations over the Fermi sea [79] (recently developed spectral algorithms could be used to mitigate this problem [90]). Bulk properties [91] can still be extracted [92] from two-terminal systems with a CA region of finite length by computing local quantities at some distance [92,93] away from the CA region/lead interface (such as at the shaded middle hexagons in Fig. 1).

To demonstrate such an equivalence, we compute the SH current (Fig. 2) and SO torque (Fig. 3) densities via Kubo and Keldysh routes for the same system—a graphene sheet with both SO coupling and magnetic ordering (Fig. 1). The effective TB Hamiltonian (whose parameters can be fitted to first-principles calculations [71] or experimental data [40]) is given by

$$\hat{H} = -t \sum_{\langle i,j\rangle,\sigma} \hat{c}^\dagger_{i\sigma}\hat{c}_{j\sigma} + \frac{2i\lambda_{\rm RSO}}{3} \sum_{\langle i,j\rangle,\sigma\neq\sigma'} [\hat{\boldsymbol{\sigma}} \times \boldsymbol{d}_{ij}]_{\sigma\sigma'}\hat{c}^\dagger_{i\sigma}\hat{c}_{j\sigma'} + \sum_{i,\sigma,\sigma'} \hat{c}^\dagger_{i\sigma}(\varepsilon_i\delta_{\sigma\sigma'} + J_{\rm sd}[\mathbf{m}_i \cdot \hat{\boldsymbol{\sigma}}]_{\sigma\sigma'})\hat{c}_{i\sigma'}. \quad (5)$$

Physically, such spin-dependent interactions can be introduced in graphene via proximity effects from an overlayer of 2D ferromagnetic insulator and underlayer of 2D semiconductor material [71]. Here, $\hat{c}^\dagger_{i\sigma}$ ($\hat{c}_{i\sigma}$) creates (annihilates) an electron at a site i with spin $\sigma = \uparrow, \downarrow$; $\hat{\boldsymbol{\sigma}} = (\hat{\sigma}_x, \hat{\sigma}_y, \hat{\sigma}_z)$ is the vector of the Pauli matrices; $t = 2.7$ eV is the nearest-neighbor (NN) hopping; the sum $\langle i, j\rangle$ goes over all pairs of NN sites; $\varepsilon_i \in [-D/2, D/2]$ is a uniform random variable introducing Anderson disorder on each site;

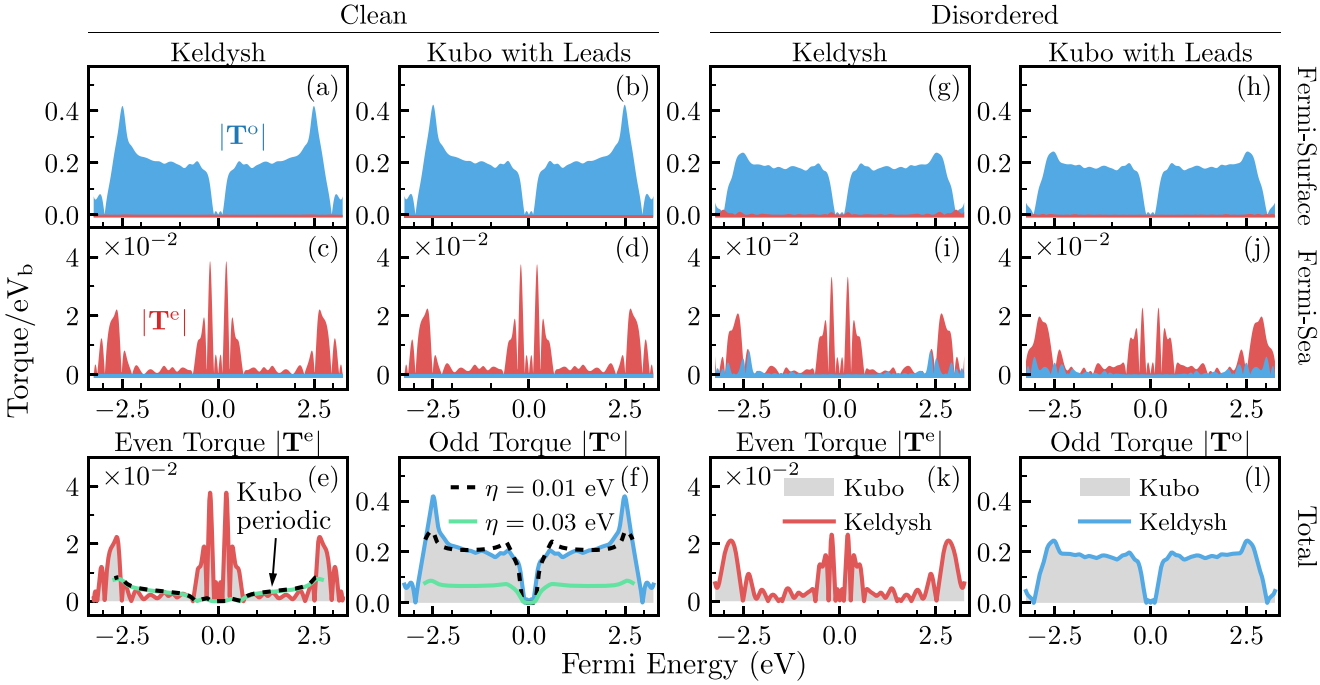

FIG. 3. Even $\mathbf{T}^e$ (or dampinglike [78,79]) and odd $\mathbf{T}^o$ (or fieldlike [78,79]) SO torques as a function of the Fermi energy. Each row was obtained by tracing the torque operator [76,79] with (a), (b), (g), (h) Fermi-surface, or (c), (d), (i), (j) Fermi-sea density matrix, as well as (e), (f), (k), (l) total density matrix within Kubo Eq. (1) vs Keldysh Eq. (4). In (a)–(f), the CA region in Fig. 1 is clean, while in (g)–(l) it contains Anderson disorder of strength $D = 0.5$ eV. (e) and (f) show additional (black and green) curves obtained from conventional [27,30–33] Kubo calculations on periodic lattices [i.e., by using Eq. (2) plugged into Eq. (1)]. The parameters in Eq. (5) read as $\lambda_{\mathrm{RSO}} = J_{\mathrm{sd}} = 0.3$ eV. Calculations with disorder employ 200 configurations.

and J_{sd} is the *sd* exchange coupling between conduction electrons and proximity-induced localized magnetic moments described by a classical unit vector $\mathbf{m}_i$. While other SO effects can be induced in graphene [71,94], we focus on the Rashba SO coupling of strength λ_{RSO}, where $\mathbf{d}_{ij}$ is the unit vector along the direction connecting NN sites i and j. The k-point sampling along the transverse direction is implemented [72] with hoppings connecting sites along the lower and upper edge of the armchair nanoribbon multiplied by the phase $e^{ik_y W}$. All results in Figs. 1(c), 2, and 3 are averaged [72,95] over the transverse wavevector using $\langle \hat{O} \rangle = W \int_{-\pi/W}^{\pi/W} dk_y \, \langle \hat{O} \rangle_{k_y} / 2\pi$. Though not essential for the Kubo versus Keldysh equivalence, the k sampling makes the system behave as infinite along the y axis and thus yields bulklike [72] behavior (considered to be the hallmark of standard [25,26,31,48] Kubo-Greenwood or Kubo-Bastin formula calculations). The infinity of our graphene sheet is demonstrated by its density of states in Fig. S1(d) of the Supplemental Material (SM) [17] being identical to standard analytical result [96], as long as a sufficient number of k_y points is included to converge.

We start the path of reconciliation by first recalling that for pure Fermi-surface transport properties, their equivalence was well-established long ago [23,63]. This has been amply confirmed [97] for, e.g., conductance [23,62,98] of two-terminal systems [99], including graphene [90,100] that we also revisit in the SM [17]. Since the conductance formulas [17] for $G_{\mathrm{Kubo}} \equiv G_{\mathrm{Keldysh}}$ are essentially the expectation value of the *total* current operator [23,63,74] in the right lead divided by the voltage drop (i.e., $G = \langle \hat{I}_R \rangle / V_b$, where $\langle \hat{I}_R \rangle = \mathrm{Tr}[\hat{\rho}^{\mathrm{surf}}_{\square} \hat{I}_R]$ and $\square =$ Kubo or $\square =$ Keldysh), this implies equivalence [23,63] of $\mathrm{Tr}[\hat{I}_R \hat{\rho}^{\mathrm{surf}}_{\mathrm{Kubo}}]$ and $\mathrm{Tr}[\hat{I}_R \hat{\rho}^{\mathrm{surf}}_{\mathrm{Keldysh}}]$ on the proviso that the retarded GF in Eq. (3) is used. This suggests that the *divergent conclusions* in recent studies of spin-dependent transport stem from attempts to calculate expectation values of *local* quantities that require additional traces of their operators with the *Fermi-sea terms*, $\hat{\rho}^{\mathrm{sea}}_{\mathrm{Kubo}}$ [Eq. (1c)] or $\hat{\rho}^{\mathrm{sea}}_{\mathrm{Keldysh}}$ [Eq. (4c)]. To investigate this issue, in Fig. 2 we first consider the expectation value of spin (Hall) current density $\langle \hat{j}^{S_z}_y \rangle$, with the corresponding operator being [92] $\hat{j}^{S_z}_y = \frac{e}{2}(\hat{v}_y \hat{\sigma}_z + \hat{\sigma}_z \hat{v}_y)$. In order to capture the bulk behavior, this local transport quantity is computed and averaged over a small area in the middle of the CA region as denoted (yellow hexagons) in Fig. 1. Note that $\langle \hat{j}^{S_z}_y \rangle$, or the SH conductivity $\sigma_{\mathrm{SH}} = \langle \hat{j}^{S_z}_y \rangle / E_x$, in the pure Rashba model (i.e., with $J_{\mathrm{sd}} = 0$) treated by the standard diagrammatic calculations with scalar disorder has zero contribution from the Fermi surface due to vertex corrections [36,39]. Interestingly, our Kubo calculations for $J_{\mathrm{sd}} \neq 0$ [gray curve in Fig. 2(a)] produce a relatively small nonzero value from the Fermi surface. The suppression of the Fermi-surface contribution to $\hat{j}^{S_z}_y$ in our results is nontrivial since the interplay of Rashba SOC and exchange coupling is expected to generate robust extrinsic spin Hall effect (SHE) via skew scattering, as shown by Boltzmann and Kubo calculations [101] (enhanced intervalley scattering due to the nature of our short-range disorder landscape [101], as well as the nondiffusive nature of our transport simulations, are likely explanations for this behavior). By contrast, the Keldysh calculations [Figs. 2(a) and 2(b)]

contain significant contributions from both the Fermi surface and Fermi sea. Although this suggests that $\hat{\rho}^{\rm surf}_{\rm Kubo} \neq \hat{\rho}^{\rm surf}_{\rm Keldysh}$ and $\hat{\rho}^{\rm sea}_{\rm Kubo} \neq \hat{\rho}^{\rm sea}_{\rm Keldysh}$, it is the sum of both contributions that carries the physical meaning. Indeed, we see that $\mathrm{Tr}[\hat{\rho}^{\rm neq}_{\rm Keldysh}\hat{j}^{\hat{S}_z}_y] \equiv \mathrm{Tr}[\hat{\rho}^{\rm neq}_{\rm Kubo}\hat{j}^{\hat{S}_z}_y]$ are perfectly matched in Fig. 2(c).

Another local transport quantity that has been a source of *divergent conclusions* is the SO torque [102]—an intensely studied phenomenon over the past decade due to its experimental [83] and technological relevance [103,104]. In general, spin torques arise [78,105] due to the exchange of spin angular momentum between flowing electrons and localized magnetization. Specifically, injected unpolarized charge current, together with SO coupling, produces nonequilibrium spin density, $\langle\hat{\mathbf{s}}_i\rangle = \mathrm{Tr}[\hat{\rho}^{\rm neq}_{\square}\hat{\boldsymbol{\sigma}}]$ where $\hat{\mathbf{s}}_i = \hat{c}^\dagger\hat{\boldsymbol{\sigma}}\hat{c}_i$ is the spin operator, whose computation makes it possible to obtain local SO torque as $\mathbf{T}_i = J_{\rm sd}\langle\hat{\mathbf{s}}_i\rangle \times \mathbf{m}_i$. Both $\square = $ Kubo [27,30–33,83–86,106] and $\square = $ Keldysh [71,75,76,79,81,82,107] density matrices have been frequently used in SO torque calculations. Similar to Fig. 2, we average the local SO torque over the middle of the CA region indicated in Fig. 1 to obtain $\mathbf{T} = \frac{1}{N}\sum_{i=1}^{N}\mathbf{T}_i = \mathbf{T}^e + \mathbf{T}^o$. Figures 3(a)–3(f) shows the energy dependence of the even and odd components of $\mathbf{T}$, with magnetization fixed out of plane $\mathbf{M} = \sum_i \mathbf{m}_i \parallel \hat{z}$, calculated for the clean system. Since both formulations in Figs. 3(a)–3(f) yield identical $\mathbf{T}^e_{\rm Kubo} \equiv \mathbf{T}^e_{\rm Keldysh}$ and $\mathbf{T}^o_{\rm Kubo} \equiv \mathbf{T}^o_{\rm Keldysh}$, this demonstrates how the Keldysh formula reproduces Fermi-sea-governed even (or dampinglike [78,79]) SO torque $\mathbf{T}^e$ in the clean limit, that was previously considered to arise only via the Kubo route [27,83–85]. In Figs. 3(e) and 3(f), we additionally show the even and odd SO torques produced by conventional usage [27,30–32] of the Kubo Eq. (1) on periodic lattices. As expected, the particular choice of the *ad hoc* broadening η affects the results for $\mathbf{T}^o$ [Fig. 3(f)], diverging with $\eta \to 0$ which is *unphysical* [81,108–110]. Moreover, $\mathbf{T}^e$ which is independent of η (and, therefore, considered "intrinsic" [83–85]), *deviates* substantially from our Kubo $\equiv$ Keldysh results for $\mathbf{T}^e$ on two-terminal systems [Fig. 3(e)]. Thus, the implementation of the Kubo(-Bastin) Eq. (1) on two-terminal geometries that we develop here evades ambiguities due to choice of η in finite-size periodic lattice calculations because two-terminal Landauer setups are infinite systems with a *continuous* energy spectrum [51] (as demanded also in the original derivations of Kubo [13,108–110]) which ensures that dissipation is effectively introduced [111–113]. Our implementation also mimics closely experimental setups where a nonequilibrium state is introduced [23,63,108–110] by injecting current through the leads or by applying a voltage difference V_b between them, rather than by applying an electric field. In the disordered case, Fig. 3(g) shows that $\hat{\rho}^{\rm surf}_{\rm Keldysh}$ produces additional contributions to the dampinglike $\mathbf{T}^e$, which we attribute to the often overlooked skew-scattering-induced dampinglike SO torque [71,86,87,114]. Also, $\hat{\rho}^{\rm sea}_{\rm Keldysh}$ and $\hat{\rho}^{\rm sea}_{\rm Kubo}$ produce [Figs. 3(i) and 3(j)] additional contributions to $\mathbf{T}^o$. Despite these differences in specific contributions, their sums produce identical results, $\mathrm{Tr}[\hat{\rho}^{\rm neq}_{\rm Keldysh}\hat{T}^{e,o}_i] \equiv \mathrm{Tr}[\hat{\rho}^{\rm neq}_{\rm Kubo}\hat{T}^{e,o}_i]$ in Figs. 3(k) and 3(l). This, together with the results of Fig. 2(c), completes our proof of equivalence.

The numerical frameworks developed and validated here demonstrate an unambiguous route to study generic spin-charge transport phenomena in the linear-response regime of realistic systems, in addition to resolving a debate in spintronics over the proper usage of Kubo and Keldysh formulas. Our findings also suggest that assigning a unique and special physical meaning [31,83–85] to the Fermi-sea term in Kubo [Eq. (1)] requires further scrutiny, as the decomposition of the density matrix into Fermi-surface and Fermi-sea contributions is not unique [17] and, as seen through the demonstrated Kubo versus Keldysh equivalence, there are many possible [17] (and rather mundane looking) forms of the Fermi-sea term within the Keldysh formalism [Eq. (4)]. The particular expression to be used in practical calculations is a matter of computational convenience [115].

B.K.N. was supported by the U.S. National Science Foundation (NSF) under Grant No. DMR-2500816. The supercomputing time was provided by DARWIN (Delaware Advanced Research Workforce and Innovation Network), which is supported by NSF Grant No. MRI-1919839. A.F. acknowledges the partial support from a Royal Society University Research Fellowship in the early stages of this project.

[1] L. E. Ballentine, *Quantum Mechanics: A Modern Development* (World Scientific, Singapore, 2014).

[2] M. Kardar, *Statistical Physics of Particles* (Cambridge University Press, Cambridge, UK, 2007).

[3] F. Nathan and M. S. Rudner, Quantifying the accuracy of steady states obtained from the universal Lindblad equation, Phys. Rev. B **109**, 205140 (2024).

[4] S. Weinberg, Quantum mechanics without state vectors, Phys. Rev. A **90**, 042102 (2014).

[5] E. Joos, H. D. Zeh, C. Kiefer, D. J. W. Giulini, J. Kupsch, and I. Stamatescu, *Decoherence and the Appearance of a Classical World in Quantum Theory* (Springer, Berlin, 2003).

[6] F. Garcia-Gaitan and B. K. Nikolić, Fate of entanglement in magnetism under Lindbladian or non-Markovian dynamics and conditions for their transition to Landau-Lifshitz-Gilbert classical dynamics, Phys. Rev. B **109**, L180408 (2024).

[7] P. Dutt, J. Koch, J. E. Han, and K. L. Hur, Effective equilibrium theory of nonequilibrium quantum transport, Ann. Phys. **326**, 2963 (2011).

[8] A. Dhar, K. Saito, and P. Hänggi, Nonequilibrium density-matrix description of steady-state quantum transport, Phys. Rev. E **85**, 011126 (2012).

[9] B. Gaury, J. Weston, M. Santin, M. Houzet, C. Groth, and X. Waintal, Numerical simulations of time-resolved quantum electronics, Phys. Rep. **534**, 1 (2014).

[10] B. S. Popescu and A. Croy, Efficient auxiliary-mode approach for time-dependent nanoelectronics, New J. Phys. **18**, 093044 (2016).

[11] U. Bajpai and B. K. Nikolić, Spintronics meets nonadiabatic molecular dynamics: Geometric spin torque and damping on dynamical classical magnetic texture due to an electronic open quantum system, Phys. Rev. Lett. **125**, 187202 (2020).

[12] M. Ridley, N. W. Talarico, D. Karlsson, N. Lo Gullo, and R. Tuovinen, A many-body approach to transport in quantum systems: From the transient regime to the stationary state, J. Phys. A: Math. Theor. **55**, 273001 (2022).

[13] R. Kubo, Statistical-mechanical theory of irreversible processes. I. General theory and simple applications to magnetic and conduction problems, J. Phys. Soc. Jpn. **12**, 570 (1957).

[14] L. Keldysh, Diagram technique for nonequilibrium processes, Sov. Phys. JETP **20**, 1018 (1965).

[15] G. Stefanucci and R. van Leeuwen, *Nonequilibrium Many-Body Theory of Quantum Systems: A Modern Introduction* (Cambridge University Press, Cambridge, UK, 2025).

[16] A. Bastin, C. Lewiner, O. Betbeder-matibet, and P. Nozieres, Quantum oscillations of the Hall effect of a fermion gas with random impurity scattering, J. Phys. Chem. Solids **32**, 1811 (1971).

[17] See Supplemental Material at http://link.aps.org/supplemental/10.1103/zwqs-gpr4, which includes Refs. [116–118], for (i) summary of different commonly employed decompositions of Kubo Eq. (1) and Keldysh Eq. (4), as well as additional details on their numerical evaluation; (ii) one additional figure recalling a well-established [23,63,99] equivalence of Kubo and Keldysh formulas for conductance (i.e., longitudinal charge transport) calculations using an example of plain [i.e., without SOC and magnetism terms in Eq. (5)] graphene in Fig. 1; and (iii) for the same plain graphene, we also show that its density of states computed using the setup of Fig. 1 is identical to standard result [96] for infinite graphene.

[18] L. Smrcka and P. Středa, Transport coefficients in strong magnetic fields, J. Phys. C: Solid State Phys. **10**, 2153 (1977).

[19] P. Streda, Theory of quantised Hall conductivity in two dimensions, J. Phys. C: Solid State Phys. **15**, L717 (1982).

[20] A. Crépieux and P. Bruno, Theory of the anomalous Hall effect from the Kubo formula and the Dirac equation, Phys. Rev. B **64**, 014416 (2001).

[21] V. Bonbien and A. Manchon, Symmetrized decomposition of the Kubo-Bastin formula, Phys. Rev. B **102**, 085113 (2020).

[22] I. A. Ado, M. Titov, R. A. Duine, and A. Brataas, Kubo formula for dc conductivity: Generalization to systems with spin-orbit coupling, Phys. Rev. Res. **6**, L012057 (2024).

[23] H. U. Baranger and A. D. Stone, Electrical linear-response theory in an arbitrary magnetic field: A new Fermi-surface formation, Phys. Rev. B **40**, 8169 (1989).

[24] D. A. Greenwood, The Boltzmann equation in the theory of electrical conduction in metals, Proc. Phys. Soc. **71**, 585 (1958).

[25] S. M. João, M. Andjelković, L. Covaci, T. G. Rappoport, J. M. V. P. Lopes, and A. Ferreira, KITE: High-performance accurate modelling of electronic structure and response functions of large molecules, disordered crystals and heterostructures, R. Soc. Open Sci. **7**, 191809 (2020).

[26] Z. Fan, J. H. Garcia, A. W. Cummings, J. E. Barrios-Vargas, M. Panhans, A. Harju, F. Ortmann, and S. Roche, Linear scaling quantum transport methodologies, Phys. Rep. **903**, 1 (2021).

[27] S. Ghosh and A. Manchon, Spin-orbit torque in a three-dimensional topological insulator–ferromagnet heterostructure: Crossover between bulk and surface transport, Phys. Rev. B **97**, 134402 (2018).

[28] D. Van Tuan, J. M. Marmolejo-Tejada, X. Waintal, B. K. Nikolić, S. O. Valenzuela, and S. Roche, Spin Hall effect and origins of nonlocal resistance in adatom-decorated graphene, Phys. Rev. Lett. **117**, 176602 (2016).

[29] J. H. Garcia, A. W. Cummings, and S. Roche, Spin Hall effect and weak antilocalization in graphene/transition metal dichalcogenide heterostructures, Nano Lett. **17**, 5078 (2017).

[30] J. Medina Dueñas, J. H. García, and S. Roche, Emerging spin-orbit torques in low-dimensional Dirac materials, Phys. Rev. Lett. **132**, 266301 (2024).

[31] F. Freimuth, S. Blügel, and Y. Mokrousov, Spin-orbit torques in Co/Pt(111) and Mn/W(001) magnetic bilayers from first principles, Phys. Rev. B **90**, 174423 (2014).

[32] F. Mahfouzi and N. Kioussis, First-principles study of the angular dependence of the spin-orbit torque in Pt/Co and Pd/Co bilayers, Phys. Rev. B **97**, 224426 (2018).

[33] F. Mahfouzi, R. Mishra, P.-H. Chang, H. Yang, and N. Kioussis, Microscopic origin of spin-orbit torque in ferromagnetic heterostructures: A first-principles approach, Phys. Rev. B **101**, 060405(R) (2020).

[34] F. J. dos Santos, D. A. Bahamon, R. B. Muniz, K. McKenna, E. V. Castro, J. Lischner, and A. Ferreira, Impact of complex adatom-induced interactions on quantum spin Hall phases, Phys. Rev. B **98**, 081407(R) (2018).

[35] E. N. Economou, *Green's Functions in Quantum Physics* (Springer, Berlin, 2006).

[36] O. V. Dimitrova, Spin-Hall conductivity in a two-dimensional Rashba electron gas, Phys. Rev. B **71**, 245327 (2005).

[37] I. A. Ado, I. A. Dmitriev, P. M. Ostrovsky, and M. Titov, Anomalous Hall effect with massive Dirac fermions, Europhys. Lett. **111**, 37004 (2015).

[38] M. Milletarì and A. Ferreira, Quantum diagrammatic theory of the extrinsic spin Hall effect in graphene, Phys. Rev. B **94**, 134202 (2016).

[39] M. Milletarì, M. Offidani, A. Ferreira, and R. Raimondi, Covariant conservation laws and the spin Hall effect in Dirac-Rashba systems, Phys. Rev. Lett. **119**, 246801 (2017).

[40] D. T. Perkins, A. Veneri, and A. Ferreira, Spin Hall effect: Symmetry breaking, twisting, and giant disorder renormalization, Phys. Rev. B **109**, L241404 (2024).

[41] Y. Imry, *Introduction to Mesoscopic Physics* (Oxford University Press, Oxford, UK, 2002).

[42] K. Nomura and A. H. MacDonald, Quantum transport of massless Dirac fermions, Phys. Rev. Lett. **98**, 076602 (2007).

[43] J. P. Santos Pires, S. M. João, A. Ferreira, B. Amorim, and J. M. Viana Parente Lopes, Anomalous transport signatures in Weyl semimetals with point defects, Phys. Rev. Lett. **129**, 196601 (2022).

[44] D. J. Thouless and S. Kirkpatrick, Conductivity of the disordered linear chain, J. Phys. C: Solid State Phys. **14**, 235 (1981).

[45] S. M. João, J. M. Viana Parente Lopes, and A. Ferreira, High-resolution real-space evaluation of the self-energy operator of disordered lattices: Gade singularity, spin–orbit effects and *p*-wave superconductivity, J. Phys. Mater. **5**, 045002 (2022).

[46] J. P. Boyd, *Chebyshev and Fourier Spectral Methods* (Dover, New York, 2000).

[47] A. Weiße, G. Wellein, A. Alvermann, and H. Fehske, The kernel polynomial method, Rev. Mod. Phys. **78**, 275 (2006).
[48] A. Ferreira and E. R. Mucciolo, Critical delocalization of chiral zero energy modes in graphene, Phys. Rev. Lett. **115**, 106601 (2015).
[49] F. M. O. Brito and A. Ferreira, Real-space spectral simulation of quantum spin models: Application to generalized Kitaev models, SciPost Phys. Core **7**, 006 (2024).
[50] P. Bulanchuk, On the delta function broadening in the Kubo-Greenwood equation, Comput. Phys. Commun. **261**, 107714 (2021).
[51] X. Waintal, M. Wimmer, A. Akhmerov, C. Groth, B. K. Nikolić, M. Istas, T. Örn Rosdahl, and D. Varjas, Computational quantum transport, arXiv:2407.16257.
[52] M. Brandbyge, J.-L. Mozos, P. Ordejón, J. Taylor, and K. Stokbro, Density-functional method for nonequilibrium electron transport, Phys. Rev. B **65**, 165401 (2002).
[53] B. K. Nikolić, S. Souma, L. P. Zârbo, and J. Sinova, Nonequilibrium spin Hall accumulation in ballistic semiconductor nanostructures, Phys. Rev. Lett. **95**, 046601 (2005).
[54] A. Reynoso, G. Usaj, and C. A. Balseiro, Spin Hall effect in clean two-dimensional electron gases with Rashba spin-orbit coupling, Phys. Rev. B **73**, 115342 (2006).
[55] P. M. Haney, D. Waldron, R. A. Duine, A. S. Núñez, H. Guo, and A. H. MacDonald, Current-induced order parameter dynamics: Microscopic theory applied to Co/Cu/Co spin valves, Phys. Rev. B **76**, 024404 (2007).
[56] D. A. Areshkin and B. K. Nikolić, *I-V* curve signatures of nonequilibrium-driven band gap collapse in magnetically ordered zigzag graphene nanoribbon two-terminal devices, Phys. Rev. B **79**, 205430 (2009).
[57] B. K. Nikolić, L. P. Zârbo, and S. Souma, Imaging mesoscopic spin Hall flow: Spatial distribution of local spin currents and spin densities in and out of multiterminal spin-orbit coupled semiconductor nanostructures, Phys. Rev. B **73**, 075303 (2006).
[58] S. A. Gulbrandsen, C. Espedal, and A. Brataas, Spin Hall effect in antiferromagnets, Phys. Rev. B **101**, 184411 (2020).
[59] Y. Imry and R. Landauer, Conductance viewed as transmission, Rev. Mod. Phys. **71**, S306 (1999).
[60] Y. V. Nazarov and Y. M. Blanter, *Quantum Transport: Introduction to Nanoscience* (Cambridge University Press, Cambridge, UK, 2009).
[61] C. Caroli, R. Combescot, P. Nozieres, and D. Saint-James, Direct calculation of the tunneling current, J. Phys. C: Solid State Phys. **4**, 916 (1971).
[62] D. S. Fisher and P. A. Lee, Relation between conductivity and transmission matrix, Phys. Rev. B **23**, 6851 (1981).
[63] H. D. Cornean, A. Jensen, and V. Moldoveanu, A rigorous proof of the Landauer–Büttiker formula, J. Math. Phys. **46**, 042106 (2005).
[64] M. C. Payne, Electrostatic and electrochemical potentials in quantum transport, J. Phys.: Condens. Matter **1**, 4931 (1989).
[65] Y. Meir and N. S. Wingreen, Landauer formula for the current through an interacting electron region, Phys. Rev. Lett. **68**, 2512 (1992).
[66] H. Ness, L. K. Dash, and R. W. Godby, Generalization and applicability of the Landauer formula for nonequilibrium current in the presence of interactions, Phys. Rev. B **82**, 085426 (2010).
[67] F. Mahfouzi and B. K. Nikolić, Signatures of electron-magnon interaction in charge and spin currents through magnetic tunnel junctions: A nonequilibrium many-body perturbation theory approach, Phys. Rev. B **90**, 045115 (2014).
[68] H. Ness and L. K. Dash, Nonequilibrium quantum transport in fully interacting single-molecule junctions, Phys. Rev. B **84**, 235428 (2011).
[69] J. Velev and W. Butler, On the equivalence of different techniques for evaluating the Green function for a semi-infinite system using a localized basis, J. Phys.: Condens. Matter **16**, R637 (2004).
[70] I. Rungger and S. Sanvito, Algorithm for the construction of self-energies for electronic transport calculations based on singularity elimination and singular value decomposition, Phys. Rev. B **78**, 035407 (2008).
[71] K. Zollner, M. D. Petrović, K. Dolui, P. Plecháč, B. K. Nikolić, and J. Fabian, Scattering-induced and highly tunable by gate damping-like spin-orbit torque in graphene doubly proximitized by two-dimensional magnet $Cr_2Ge_2Te_6$ and monolayer WS_2, Phys. Rev. Res. **2**, 043057 (2020).
[72] M.-H. Liu and K. Richter, Efficient quantum transport simulation for bulk graphene heterojunctions, Phys. Rev. B **86**, 115455 (2012).
[73] M. O. A. Ellis, M. Stamenova, and S. Sanvito, Multiscale modeling of current-induced switching in magnetic tunnel junctions using *ab initio* spin-transfer torques, Phys. Rev. B **96**, 224410 (2017).
[74] F. Mahfouzi and B. K. Nikolić, How to construct the proper gauge-invariant density matrix in steady-state nonequilibrium: Applications to spin-transfer and spin-orbit torques, SPIN **03**, 1330002 (2013).
[75] F. Mahfouzi, B. K. Nikolić, and N. Kioussis, Antidamping spin-orbit torque driven by spin-flip reflection mechanism on the surface of a topological insulator: A time-dependent nonequilibrium Green function approach, Phys. Rev. B **93**, 115419 (2016).
[76] B. K. Nikolić, K. Dolui, M. Petrović, P. Plecháč, T. Markussen, and K. Stokbro, First-principles quantum transport modeling of spin-transfer and spin-orbit torques in magnetic multilayers, in *Handbook of Materials Modeling*, edited by W. Andreoni and S. Yip (Springer, Cham, 2018), pp. 1–35.
[77] I. Theodonis, N. Kioussis, A. Kalitsov, M. Chshiev, and W. H. Butler, Anomalous bias dependence of spin torque in magnetic tunnel junctions, Phys. Rev. Lett. **97**, 237205 (2006).
[78] D. Ralph and M. Stiles, Spin transfer torques, J. Magn. Magn. Mater. **320**, 1190 (2008).
[79] K. D. Belashchenko, A. A. Kovalev, and M. van Schilfgaarde, First-principles calculation of spin-orbit torque in a Co/Pt bilayer, Phys. Rev. Mater. **3**, 011401(R) (2019).
[80] E. I. Rashba, Spin currents in thermodynamic equilibrium: The challenge of discerning transport currents, Phys. Rev. B **68**, 241315(R) (2003).
[81] A. Kalitsov, S. A. Nikolaev, J. Velev, M. Chshiev, and O. Mryasov, Intrinsic spin-orbit torque in a single-domain nanomagnet, Phys. Rev. B **96**, 214430 (2017).
[82] K. Dolui, M. D. Petrović, K. Zollner, P. Plecháč, J. Fabian, and B. K. Nikolić, Proximity spin-orbit torque on a two-dimensional magnet within van der Waals heterostructure: Current-driven antiferromagnet-to-ferromagnet

reversible nonequilibrium phase transition in bilayer CrI_3, Nano Lett. **20**, 2288 (2020).

[83] H. Kurebayashi, J. S. D. Fang, A. C. Irvine, T. D. Skinner, J. Wunderlich, V. Novák, R. P. Campion, B. L. Gallagher, E. K. Vehstedt, L. P. Zârbo, K. Výborný, A. J. Ferguson, and T. Jungwirth, An antidamping spin-orbit torque originating from the Berry curvature, Nat. Nanotechnol. **9**, 211 (2014).

[84] K.-S. Lee, D. Go, A. Manchon, P. M. Haney, M. D. Stiles, H.-W. Lee, and K.-J. Lee, Angular dependence of spin-orbit spin-transfer torques, Phys. Rev. B **91**, 144401 (2015).

[85] H. Li, H. Gao, L. P. Zârbo, K. Výborný, X. Wang, I. Garate, F. Doğan, A. Čejchan, J. Sinova, T. Jungwirth, and A. Manchon, Intraband and interband spin-orbit torques in noncentrosymmetric ferromagnets, Phys. Rev. B **91**, 134402 (2015).

[86] F. Sousa, G. Tatara, and A. Ferreira, Skew-scattering-induced giant antidamping spin-orbit torques: Collinear and out-of-plane Edelstein effects at two-dimensional material/ferromagnet interfaces, Phys. Rev. Res. **2**, 043401 (2020).

[87] A. Veneri, D. T. S. Perkins, and A. Ferreira, Nonperturbative approach to interfacial spin-orbit torques induced by the Rashba effect, Phys. Rev. B **106**, 235419 (2022).

[88] K. Garello, I. M. Miron, C. O. Avci, F. Freimuth, Y. Mokrousov, S. Blügel, S. Auffret, O. Boulle, G. Gaudin, and P. Gambardella, Symmetry and magnitude of spin–orbit torques in ferromagnetic heterostructures, Nat. Nanotechnol. **8**, 587 (2013).

[89] Note that many Keldysh density matrix-based studies of current-driven $\langle \hat{\mathbf{s}}_i \rangle$ [54,119] or thereby induced spin torque [55,81] in a two-terminal Landauer setup use only $\rho^{\rm surf}_{\rm Keldysh}$ [Eq. (4b)], while evading computation of $\rho^{\rm sea}_{\rm Keldysh}$ [Eq. (4c)], which can produce results *violating* the gauge invariance [74,120].

[90] S. G. de Castro, J. M. Viana Parente Lopes, A. Ferreira, and D. A. Bahamon, Fast Fourier-Chebyshev approach to real-space simulations of the Kubo formula, Phys. Rev. Lett. **132**, 076302 (2024).

[91] Note that there is widespread (but incorrect in the light of our study) perception that only the Kubo(-Bastin) formula evaluated for periodic lattices yields bulk quantities, while the Keldysh formula is needed for nonperiodic junctions with interfaces [119].

[92] L. Wang, R. J. H. Wesselink, Y. Liu, Z. Yuan, K. Xia, and P. J. Kelly, Giant room temperature interface spin Hall and inverse spin Hall effects, Phys. Rev. Lett. **116**, 196602 (2016).

[93] K. D. Belashchenko, G. G. Baez Flores, W. Fang, A. A. Kovalev, M. van Schilfgaarde, P. M. Haney, and M. D. Stiles, Breakdown of the drift-diffusion model for transverse spin transport in a disordered Pt film, Phys. Rev. B **108**, 144433 (2023).

[94] D. T. S. Perkins and A. Ferreira, Spintronics in 2D graphene-based van der Waals heterostructures, in *Encyclopedia of Condensed Matter Physics*, edited by T. Chakraborty (Academic Press, Oxford, UK, 2024), pp. 205–222.

[95] K. S. Thygesen and K. W. Jacobsen, Interference and k-point sampling in the supercell approach to phase-coherent transport, Phys. Rev. B **72**, 033401 (2005).

[96] A. H. Castro Neto, F. Guinea, N. M. R. Peres, K. S. Novoselov, and A. K. Geim, The electronic properties of graphene, Rev. Mod. Phys. **81**, 109 (2009).

[97] Nevertheless, confusion occasionally arises in the literature, such as in Fig. 6 of Ref. [26] where the Kubo conductivity incorrectly does not match quantized conductance from the Keldysh approach.

[98] C. L. Kane, R. A. Serota, and P. A. Lee, Long-range correlations in disordered metals, Phys. Rev. B **37**, 6701 (1988).

[99] B. K. Nikolić, Deconstructing Kubo formula usage: Exact conductance of a mesoscopic system from weak to strong disorder limit, Phys. Rev. B **64**, 165303 (2001).

[100] S. G. de Castro, A. Ferreira, and D. A. Bahamon, Efficient Chebyshev polynomial approach to quantum conductance calculations: Application to twisted bilayer graphene, Phys. Rev. B **107**, 045418 (2023).

[101] M. Offidani and A. Ferreira, Anomalous Hall effect in 2D Dirac materials, Phys. Rev. Lett. **121**, 126802 (2018).

[102] A. Manchon, J. Železný, I. M. Miron, T. Jungwirth, J. Sinova, A. Thiaville, K. Garello, and P. Gambardella, Current-induced spin-orbit torques in ferromagnetic and antiferromagnetic systems, Rev. Mod. Phys. **91**, 035004 (2019).

[103] N. Locatelli, V. Cros, and J. Grollier, Spin-torque building blocks, Nat. Mater. **13**, 11 (2014).

[104] W. A. Borders, H. Akima, S. Fukami, S. Moriya, S. Kurihara, Y. Horio, S. Sato, and H. Ohno, Analogue spin-orbit torque device for artificial-neural-network-based associative memory operation, Appl. Phys. Express **10**, 013007 (2017).

[105] M. D. Petrović, P. Mondal, A. E. Feiguin, P. Plecháč, and B. K. Nikolić, Spintronics meets density matrix renormalization group: Quantum spin-torque-driven nonclassical magnetization reversal and dynamical buildup of long-range entanglement, Phys. Rev. X **11**, 021062 (2021).

[106] I. A. Ado, O. A. Tretiakov, and M. Titov, Microscopic theory of spin-orbit torques in two dimensions, Phys. Rev. B **95**, 094401 (2017).

[107] K. D. Belashchenko, A. A. Kovalev, and M. van Schilfgaarde, Interfacial contributions to spin-orbit torque and magnetoresistance in ferromagnet/heavy-metal bilayers, Phys. Rev. B **101**, 020407(R) (2020).

[108] J. Wu and M. Berciu, Kubo formula for open finite-size systems, Europhys. Lett. **92**, 30003 (2010).

[109] A. Kundu, A. Dhar, and O. Narayan, The Green–Kubo formula for heat conduction in open systems, J. Stat. Mech. (2009) L03001.

[110] N. Kamiya and S. Takesue, Kubo formula for finite open quantum systems, J. Phys. Soc. Jpn. **82**, 114002 (2013).

[111] G. Giuliani and G. Vignale, *Quantum Theory of the Electron Liquid* (Cambridge University Press, Cambridge, UK, 2008).

[112] M. D. Petrović, B. S. Popescu, U. Bajpai, P. Plecháč, and B. K. Nikolić, Spin and charge pumping by a steady or pulse-current-driven magnetic domain wall: A self-consistent multiscale time-dependent quantum-classical hybrid approach, Phys. Rev. Appl. **10**, 054038 (2018).

[113] J. Varela-Manjarres and B. K. Nikolić, High-harmonic generation in spin and charge current pumping at ferromagnetic or antiferromagnetic resonance in the presence of spin-orbit coupling, J. Phys. Mater. **6**, 045001 (2023).

[114] J. Y. Zhang, P. W. Dou, R. Y. Liu, Y. B. Wang, X. Deng, L. Y. Feng, X. Q. Zheng, H. Huang, and S. G. Wang, Enhanced spin orbit torque efficiency induced by large skew scattering in perpendicular Pt/Co/Ta multilayers with superlattice/alloying Nb (Ir) insertion, Appl. Phys. Lett. **123**, 182401 (2023).

[115] Note that in the "symmetrized decomposition" of Ref. [21], the integrand in Eq. (1c) is not analytic in the upper complex

plane, which introduces additional computational complexity. In some other decompositions, and for the integration in Eq. (4c), many efficient complex contour-based algorithms have been developed [52,121,122]; see the SM [17] for more details.

[116] S. Mousavi, J. Pask, and N. Sukumar, Efficient adaptive integration of functions with sharp gradients and cusps in n-dimensional parallelepipeds, Int. J. Numer. Methods Eng. **91**, 343 (2012).

[117] T. Ando, Quantum point contacts in magnetic fields, Phys. Rev. B **44**, 8017 (1991).

[118] P. A. Khomyakov, G. Brocks, V. Karpan, M. Zwierzycki, and P. J. Kelly, Conductance calculations for quantum wires and interfaces: Mode matching and Green's functions, Phys. Rev. B **72**, 035450 (2005).

[119] A. Fabian, M. Czerner, C. Heiliger, H. Rossignol, M.-H. Wu, and M. Gradhand, Spin accumulation from nonequilibrium first principles methods, Phys. Rev. B **104**, 054402 (2021).

[120] T. Christen and M. Büttiker, Gauge-invariant nonlinear electric transport in mesoscopic conductors, Europhys. Lett. **35**, 523 (1996).

[121] T. Ozaki, Continued fraction representation of the Fermi-Dirac function for large-scale electronic structure calculations, Phys. Rev. B **75**, 035123 (2007).

[122] D. A. Areshkin and B. K. Nikolić, Electron density and transport in top-gated graphene nanoribbon devices: First-principles Green function algorithms for systems containing a large number of atoms, Phys. Rev. B **81**, 155450 (2010).